Author/s:
Abu-Zidan, Y;Rathnayaka, S;Mendis, P;Nguyen, K

Title:
Effect of wind speed and direction on facade fire spread in an isolated rectangular building

Date:
2022-05-01

Citation:
Abu-Zidan, Y., Rathnayaka, S., Mendis, P. & Nguyen, K. (2022). Effect of wind speed and direction on facade fire spread in an isolated rectangular building. Fire Safety Journal, 129, https://doi.org/10.1016/j.firesaf.2022.103570.

Persistent Link:
https://hdl.handle.net/11343/299894

Accepted for publication in ***Fire Safety Journal*** (March 17, 2022)
https://doi.org/10.1016/j.firesaf.2022.103570

Effect of wind speed and direction on facade fire spread in an isolated rectangular building

Yousef Abu-Zidan[a,b]*, Shyanaka Rathnayaka[b], Priyan Mendis[b], Kate Nguyen[a]

[a] Civil and Infrastructure Engineering, RMIT University, VIC 3001, Australia
[b] Department of Infrastructure Engineering, University of Melbourne, VIC 3010, Australia
* Corresponding author. Email address: yousef.abu-zidan@rmit.edu.au

Abstract

This paper investigates the influence of wind speed and direction on external fire spread in an isolated rectangular building using computational fluid dynamics models validated with wind tunnel data and facade fire tests. Two wind speeds (2 m/s, 4 m/s) are considered for each of four wind directions (0°, 45°, 90°, 180°) and compared to a reference case of no wind. Results indicate that facade fire spread is heavily influenced by the near-wall flow fields generated by the building geometry. These flow fields explain counterintuitive findings such as the upstream tilting of flames under the influence of reverse flow near the side walls. The presence of external wind was found to inhibit the initial development of facade fires, but can greatly exacerbate fire spread once the fire has fully developed. The largest fire occurred for the case of no wind (7.5 GJ in 15 min) while the smallest fire occurred for the 4m/s diagonal wind case (2.2 GJ). An additional case with temporally varying wind conditions demonstrated a 50% increase in fire spread area compared to no wind. The study provides valuable insight into wind and fire interaction in building facades that can help improve the fire safety of buildings.

Keywords

External wind; facade fire; combustible cladding; CFD simulation; near-wall reverse flow; synergistic effect; external flame spread

1 Introduction

Recent incidents around the world have demonstrated the potentially devastating impact that combustible cladding can have on the loss of life and property [1]. Modern trends towards environmental sustainability and energy efficiency have resulted in the use of combustible facade materials that are highly vulnerable to fire. Every year, an average of five tall buildings experience fire spread along the external facade [2], with recent events such as the Grenfell Tower fire in London, UK [3, 4] (Figure 1) and the Lacrosse fire in Melbourne, Australia [5] demonstrating the significant influence that combustible facade materials can have on the speed of fire propagation along the external walls of the building.

Figure 1: Recent example of combustible facade fires in Grenfell Tower, London, UK on 14 June 2017.

Although it is known that wind has a considerable effect on the spread of urban fires [6-9], the nature of wind and fire interaction in facade fire propagation is yet to be investigated in detail. Current standards for testing the fire performance of external facade systems, such as the ISO 13785 [10], BS 8414-1 [11], and AS 5113 [12], acknowledge the influence of external wind on large scale fire tests and hence require wind speed at the beginning of testing to not exceed a maximum limit in order to ensure consistency of results. The standards however do not require testing to be performed for different wind speeds and directions. This results in uncertainty regarding the real-life performance of facade systems under external wind.

Recent studies on ejected facade flames indicate that wind can influence facade fires in two main ways: it can affect the flame height and trajectory, and it can affect the heat release rate of the fire. Wind acting perpendicular to the facade was seen to reduce the height of ejected flames [13, 14], while wind acting parallel to the facade was seen to tilt the ejected flame towards the downwind direction [15-19]. The tilting angle increases with wind speed, and for very strong winds, the fire may even spread horizontally along the same floor. This has been shown to reduce the effectiveness of fire protection features such as overhangs and balconies that are designed to block vertical overflow of fire plume spread [20]. The tilted trajectory of the flame allows the fire to penetrate the space between balconies and overhangs, leading to vertical fire spread to upper floors.

The presence of external wind is also reported to influence the temperature and heat release rate of facade fires. Hu et al. [13] mention two competing effects when subjecting a window-ejected flame to external wind: the “air supply effect” and the “venting effect”. Below a certain threshold of wind speed, the presence of external wind increases the air supply to the fire and consequently increases the heat release rate. In such a case, the air supply effect is said to be dominant. As the wind speed exceeds the threshold, the venting effect becomes dominant where the presence of external wind causes unburnt fuel vapours to be vented away from the heat source before being ignited. Under such

conditions, an increase in wind speed will result in a reduction of heat release rate and flame temperature.

The competing interaction between the air supply and venting effects help explain seemingly conflicting findings in the literature. Wind acting perpendicular [21, 22] and parallel [17] to the facade was reported to reduce the temperature of window-ejected flames, while an outdoor experiment by Anderson et al. [22] reports an increase in fuel consumption on days when wind speed was higher. The interaction of wind and fire is further complicated by various parameters including the size and geometric configuration of facade openings and the presence of cross ventilation [23-26].

Previous studies on wind and fire interaction have mostly focused on window-ejected flames. Studies on fire propagation along the external building walls are scarce and mostly consider fire spread on a localised facade section [27] without accounting for the effect of the wind flow structures generated by the full building geometry. The presence of a building in a wind flow stream generates complex flow patterns that vary considerably from those experienced by a thin facade section. These flow structures dictate the wind conditions at various locations on the building surface and can therefore influence the spread of facade fires. The main flow structures generated by a rectangular building are shown in Figure 2 and include the following features:

- **Stagnation region**. This region forms in front of windward surfaces where wind flow is blocked by the presence of the building. The region is characterised by low wind speed and large positive pressures. For tall buildings, a downdraft may occur along the windward surface as high wind speed at the top of the building is diverted downwards.
- **Wake region.** Flow separation at the leading edges of the building results in the formation of a wake region that encompasses the top, side, and leeward surfaces. The wake region is characterised by high turbulence, low wind speed, and negative pressure. Vortex shedding may also occur in the wake region, particularly for tall and slender buildings.
- **Wind shear layers**. Flow separation at the leading edges results in the formation of wind shear layers that define the boundary between the undisturbed streamwise flow and the wake regions. Shear layers are characterised by high wind speeds and a large velocity gradient. The trajectory of these layers is highly unstable, and very large negative pressures occur immediately downstream of the point of separation where shear layers originate.

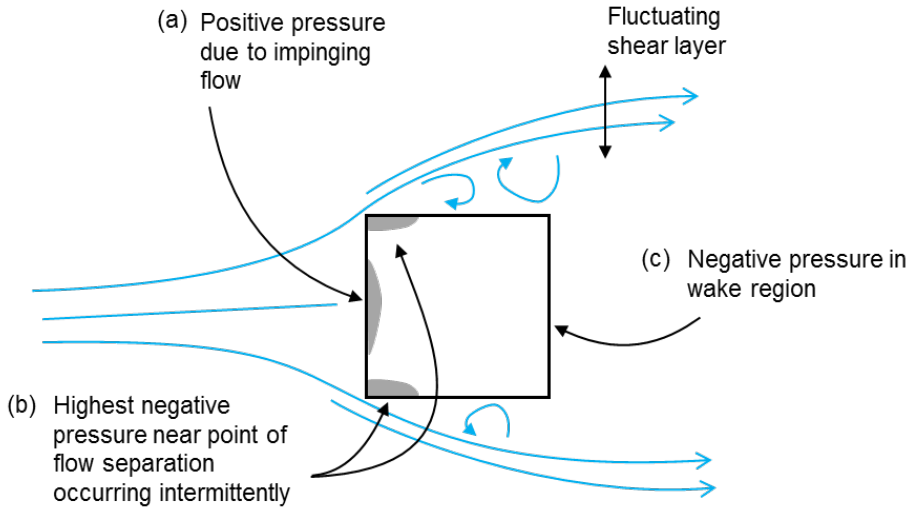

Figure 2: Top view of wind flow past a rectangular building. Wind flow direction from left to right [28].

A fire travelling along the building facade may experience varying wind conditions as it moves through the different wind flow structures generated by the building. These conditions also vary temporally due to flow instability caused by atmospheric and building-generated turbulence as well as changes in weather conditions. Such effects need to be considered when predicting fire propagation along building facades.

This paper presents a systematic investigation of the influence of wind flow patterns generated by an isolated rectangular building on the propagation of fire along the external facade. The study is performed using computational fluid dynamics (CFD) simulations that are validated with wind tunnel data and facade fire tests. Fire Dynamics Simulator (FDS) 6.7.5 is used to simulate both the wind flow field and facade fire propagation. The study involves the following steps:

1. Validating the wind flow field in FDS with results from the wind tunnel.
2. Validating the fire properties of the combustible facade material in FDS with results from facade fire tests.
3. Performing a parametric study that involves varying the wind speed and wind direction relative to the fire source on the building facade.

The findings of this study provide valuable insight into wind and fire interaction in building facades that can help improve fire safety of buildings.

2 Methodology and numerical setup

The use of computational wind engineering (CWE) principles and tools for fire safety applications has gained recent interest [6], and best practice guidelines for developing wind and fire coupled modelling have been developed [29]. Developing a CWE model involves defining a building geometry within a computational domain and specifying appropriate boundary conditions and meshing parameters. These details are specified as follows.

2.1 Building geometry and wind profile

An isolated rectangular building with height H = 20 m and width B = 10 m is adopted in this study. The building is subjected to an atmospheric boundary layer profile with reference wind speeds corresponding to highly recurrent winds. Wind speed in FDS is specified in terms of the logarithmic law [Eq. (1)]. The highest wind speed in this study is U_{ref} = 4 m/s at z_{ref} of 10 m. Open terrain roughness is selected (z_0 = 0.01 m) and von Karman constant κ is equal to 0.4. Inflow turbulence is ignored in this study to reduce complexity and computational cost.

$$U = \frac{u_*}{\kappa} \ln\left(\frac{z}{z_0}\right) \quad (1)$$

For each simulation case, the selected wind speed and direction is held constant for the entire duration of the simulation. Later in section 6.6, additional cases are presented where wind speed and direction are varied during the simulation to investigate the effect of variable wind conditions on facade fire propagation.

2.2 Mesh configurations and domain size

Fire analysis requires mesh refinement in the region of the fire plume, which in this study is located near the building surfaces. The recommended grid size is estimated using the following equation [30]:

$$D^* = \left(\frac{\dot{Q}}{\rho_\infty c_p T_\infty \sqrt{g}}\right)^{2/5} \quad (2)$$

where D^* is the characteristic fire diameter, $\dot{Q}$ is the total heat release rate of the fire, ρ_∞ is the air density, $c_p$is the specific heat of air, T_∞ is the ambient temperature, and g is gravity. A grid with D^*/δ_X between 4 and 16 is desirable, where δ_X is the nominal size of the mesh cell. Using Eq. (2), an acceptable grid size in the current study is 0.25 m for a fire heat release rate of 3.4 MW. The resulting D^*/δ_X value is around 6 which falls within the acceptable range.

A high level of mesh resolution near the building is also needed for better resolution of wind flow features. To reduce the total number of computational elements, selective refinement is specified near the building surface while coarser elements are specified elsewhere in the domain. Using a blocking technique, a structured cartesian grid is generated with 0.25 m elements near the building surfaces, a maximum element size of 2m away from the building (Figure 3). The total cell count is 1.7 million elements.

The size of the computational domain is minimised to limit the total number of cells in the model. It is important to note that wind flow simulations generally require large computational domains to ensure appropriate development of the flow field around the building with minimal influence from domain boundaries [31, 32]. However, adopting a large domain in the current study was found to be computationally prohibitive. FDS requires the use of highly structured grids with stringent requirements for grid alignment in all directions, and this low level of mesh control makes it very difficult to limit the number of computational elements in large domains through selective refinement. The computational domain in this study has an upstream and downstream length = $2H$, side clearances = $2H$ and domain height = $2H$ (Figure 3).

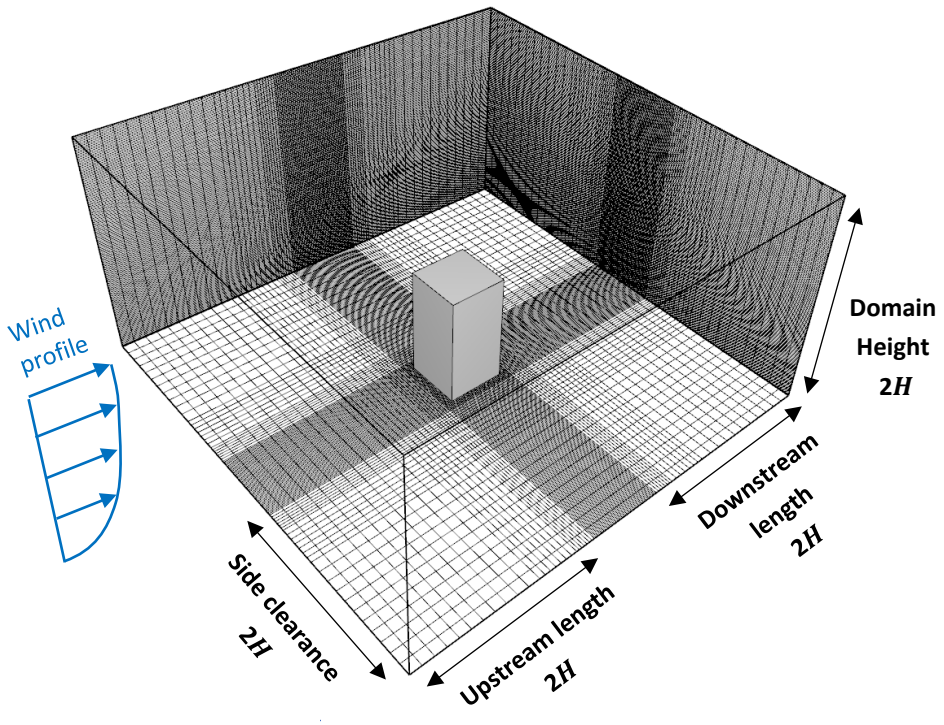

Figure 3: Mesh configuration with increasing refinement near the building. Mesh count is 1.7 million elements.

2.3 Turbulence modelling and near-wall treatment

Flow turbulence is resolved using large-eddy simulations (LES) with the Smagorinsky sub-grid scale model [33] and the default value of model constant Cs = 0.2. The Smagorinsky model has been shown to perform reasonably well for predicting wind flow around a rectangular building of similar aspect ratio to the current study [34]. A wall boundary condition is specified at the ground and building surfaces, while a velocity inlet condition is specified at the lateral boundary corresponding to the wind approach direction. All other lateral boundaries, as well as the top boundary, are specified open boundary conditions. At the building surface, near-wall flow is treated using wall functions based on the logarithmic law of the wall [35]. The wall functions are used for determining the wall stresses (τ_w), while the eddy viscosity (μ_t) in the wall-adjacent cells are determined using the wall-adapting local eddy-viscosity (WALE) model [36].

3 Validating wind flow field in FDS

The wind flow field is validated by comparing results from FDS to experimental results from the wind tunnel. The experimental results of Meng and Hibi [37] are used which provide wind speed measurements at various locations around a rectangular building (height to width ratio of 2:1) subjected to an atmospheric wind profile. The inflow wind speed profile in FDS is selected to closely reflect the wind profile from in the wind tunnel experiment. The FDS profile is defined in terms of the logarithmic law [Eq. (1)], with u_*= 0.24 m/s, κ = 0.4, and an aerodynamic roughness length of z_0 = 0.01 m. This corresponds to a reference windspeed U_{ref} = 4 m/s at the reference height z_{ref} = 10 m. A good agreement between the numerical and experimental profile is observed as shown in Figure 4.

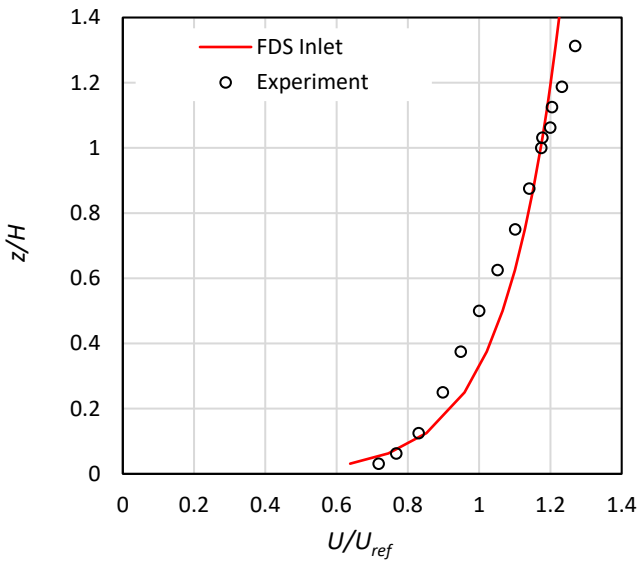

Figure 4: Comparison of wind speed profile in FDS simulation and wind tunnel experiment [37].

To validate the numerical model, wind speed is measured in the FDS model at 186 locations around the building. The locations of these measurements are specified in Meng and Hibi [37]. Computations are performed for 100 s to initialise the flow field and a further 300 s over which time histories of wind speeds are recorded. Mean wind speeds at each measurement location is calculated by averaging the time history signal and the results are compared with experiments in Figure 5, where the vertical axis corresponds to numerical results from FDS, the horizontal axis corresponds to experimental results, and the shaded areas show the error margins. The dashed diagonal line represents an exact correlation between experimental and numerical results, and the data is fitted with a linear regression curve (red line) with intercepts set at 0.

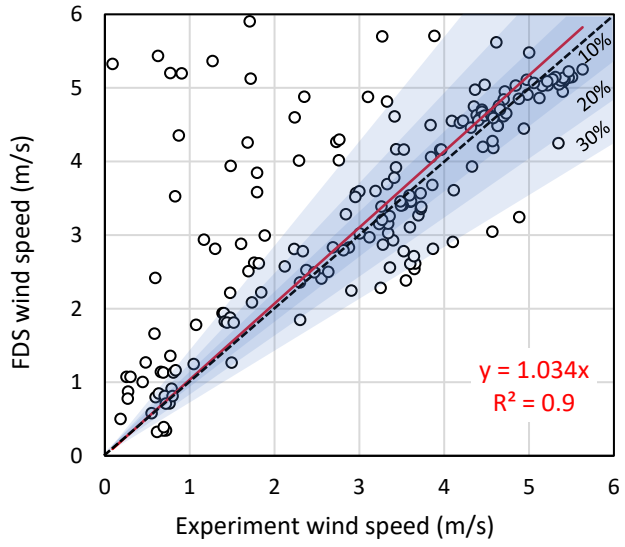

Figure 5: Comparison of FDS wind speed predictions with experimental results [37] with shaded areas showing error margin.

The results in Figure 5 indicate an acceptable level of agreement between the FDS model and experiment where 70% of all predictions fell within an error margin of ±30%. The R-squared value (coefficient of determination) is 0.9 and the linear regression slope is almost equal to 1.

Nonetheless, some noticeable discrepancies occur at a limited number of locations in Figure 5 where the wind speed was overpredicted by the FDS model. These problematic points occur mostly at the boundary of the wake region and near the edge-induced shear layer, which suggests that the discrepancies are due to the FDS model underpredicting the size of the wake region. The FDS model seems to predict a narrower wake with the shear layers located closer to the sides of the building compared to the experiment. The exact cause of this error is not immediately evident and could be due to several factors including insufficient mesh refinement and lack of inflow turbulence. The relatively small domain size may have also contributed to the narrower wake and acceleration of flow near the sides of the building [32]. Aside from these discrepancies, the FDS model performed reasonably well at other locations near the building surface with a mean absolute error of 27%.

To further validate the FDS model, a qualitative investigation of the wind flow field around the building is performed. Figure 6 presents contour plots of instantaneous wind speeds on the central vertical plane (Figure 6a) and a horizontal plane at the mid-height of the building (Figure 6b). These plots confirm the formation of wind flow structures that include a stagnation region at the windward surface, a wake region on the sides and leeward faces, and fluctuating shear layers at the leading edges of the building. These structures are consistent with those observed around an isolated rectangular building in previous wind tunnel experiments and numerical studies. Hence, the FDS model is deemed adequate for the purposes of investigating wind and fire interaction in building facades, despite some inaccuracies in the quantitative prediction of wind speeds at a limited number of locations in the model.

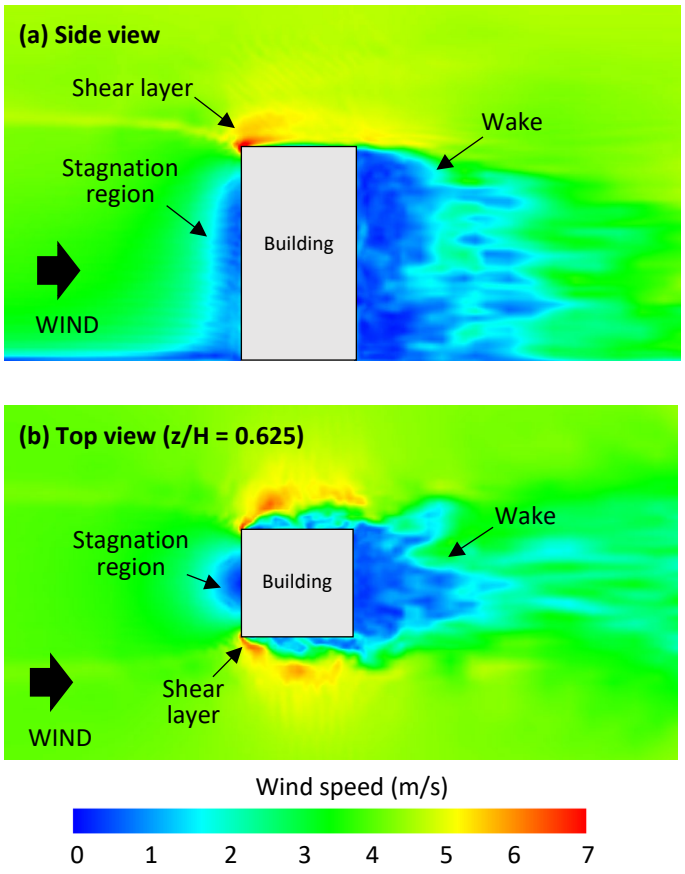

Figure 6: Side view (a) and top view (b) of the instantaneous wind flow field around the building from the FDS model.

4 Validating combustion properties of facade material

Before investigating wind and fire interaction, a numerical model for the cladding material is developed in FDS and validated with experimental data. Aluminium composite panels (ACP) with a polyethene (PE) core was selected for this study due to their high combustibility and readily available experimental data on fire performance. Large-scale experimental testing of various ACPs was commissioned by the Department for Communities and Local Government (DCLG), London in response to the Grenfell cladding fire incident. Testing was performed per the BS 8414-1 standard for assessing the behaviour of non-load bearing external cladding systems exposed to an external fire [11]. The material from DCLG fire test 1 [38] is selected in this study (Figure 7), which consists of a front-facing aluminium composite panel (ACP) constructed from two 0.5 mm aluminium sheets that surround a 3 mm PE core on either side. A 55 mm air gap is provided behind the ACP, followed by a 100 mm-thick rigid polyisocyanurate foam (PIR) insulation board.

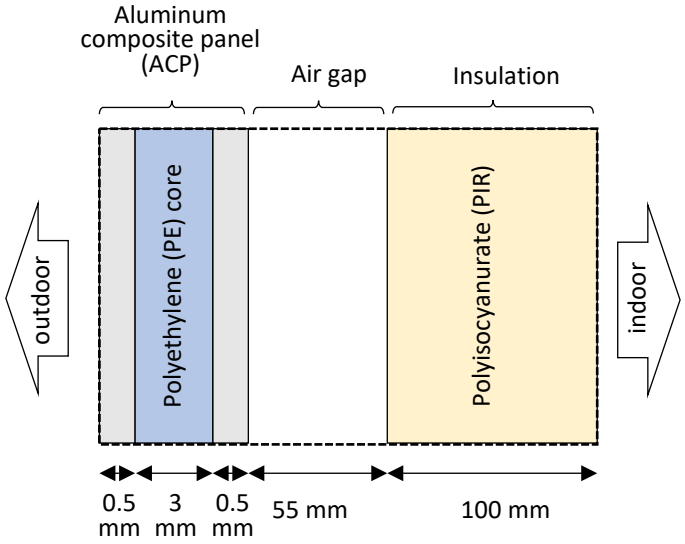

Figure 7: Cladding cross-section showing material composition and thicknesses.

Figure 8a shows the DCLG testing rig. The cladding extends 8.5 m high (6.5 m above fire source), and the widths of the main wall and wing wall are 2.6 m and 1.3 m, respectively. Thermocouples are installed at two levels with heights of 2.5 m and 5 m above the fire source.

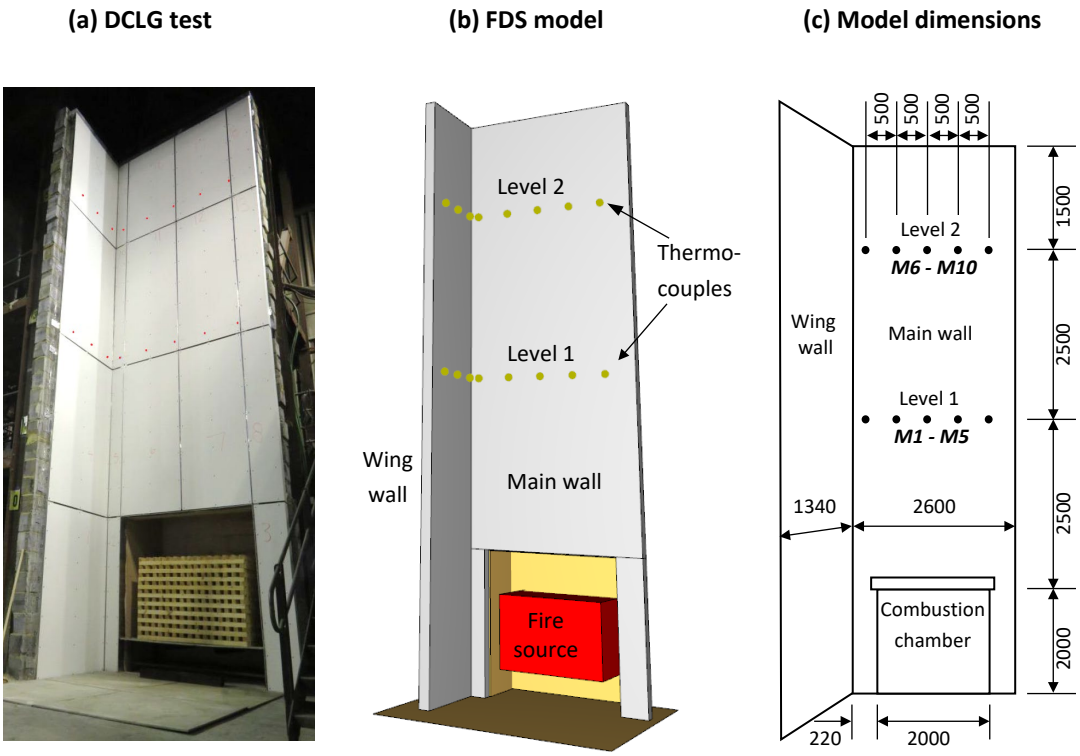

Figure 8: (a) Full-scale DCLG test [38], (b) equivalent FDS model, and (c) model dimensions in mm (not to scale).

To validate the material properties in the numerical model, an equivalent testing rig is constructed in FDS (Figure 8b) with equivalent locations of thermocouples and an equivalent fire source. Combustion properties of the ACP material were selected by calibrating the FDS model to experimental measurement from the cladding fire test. A computational grid of 0.25m is used which is equivalent to that adopted in the full building model. Although this grid is quite coarse considering the scale of the testing rig, maintaining a consistent grid between the fire rig model (Figure 8b) and the full building model (Figure 3) was necessary as previous studies have demonstrated that the computational grid can influence combustion behaviour of materials [39]. Having a consistent grid will ensure that calibrated material is appropriate for use in the full building model.

4.1 Fire source properties

The fire source in the DCLG test is based on BS 8414-1 specification represents an external fire source, or a fully-developed fire in a room, that exposes the cladding to external flame [38]. The fire source in the cladding experiment involves a wooded crib with approximate dimensions of 1.5 m x 1 m x 1 m. Figure 9 shows the heat release rate function of the wooden crib which was calibrated by Dréan et al. [39]. The fire source has a maximum heat release rate of approximately 3.4 MW.

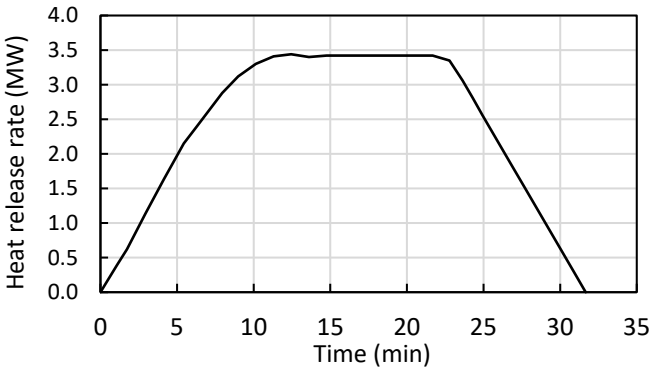

Figure 9: Heat release rate of fire source [39].

4.2 Thermal properties of facade material

Simulating ACP material in FDS is challenging as this material consists of multiple layers with varying combustion and thermal properties. The thermal properties of the ACP components are listed in Table 1.

Table 1: Thermal properties of ACP materials [40-42]

Material	**Aluminium**	**Polyethylene (PE)**	**Polyisocyanurate (PIR)**	**Air gap**
Density (kg/m^3)	2700	1360	36	1.2
Specific heat (J/g K)	0.9	2	1.1	0.85
Thermal conductivity (W/m K)	237	0.43	0.048	-
Emissivity	0.7	0.9	1	0.8

A challenging aspect of modelling ventilated cladding is accounting for the insulating air layer between the exterior facade panel and internal insulation. Earlier studies have modelled the air gap explicitly by providing computational cells across the air gap and specifying two distinct surfaces to model the external panel and internal insulation [39, 40]. This approach is however computationally restrictive in the current study because the entire building is simulated and not just a portion of the facade. Explicitly modelling flow in the narrow air gap between the exterior panel and insulation requires a very fine grid which considerably increases the number of computational cells. Also, a smaller timestep is needed to ensure solver stability which greatly increases computational cost.

Hence, an alternative approach is adopted where the air gap is modelled with a solid material with thermal properties equivalent to those expected in an air gap. This approach was proposed by Drean et al. [43] who derived an expression for equivalent thermal conductivity that accounts for the total heat transfer across the air gap due to the combined effect of convection, conduction, and radiation. Figure 10 presents the thermal conductivity function for a 55 mm air gap adopted in this study.

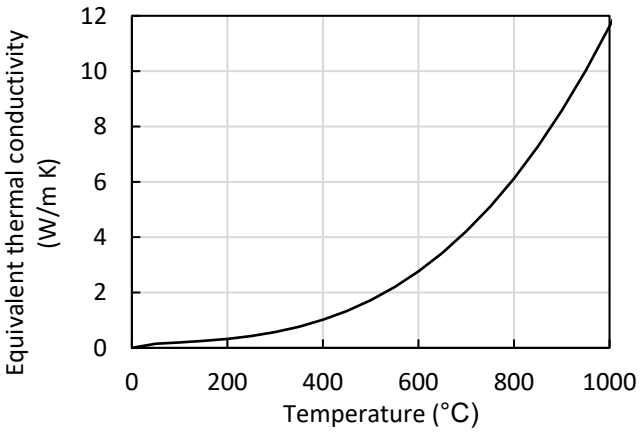

Figure 10: Equivalent thermal conductivity of 55 mm air gap as a function of the average temperature in the air gap

It should be noted that the treatment of the air gap as a solid layer, rather than explicit modelling of airflow in the gap, will result in considerable limitations such as the exclusion of the stack (chimney) effect from the analysis, and also the exclusion of the insulation combustion effect and the effect of cavity barriers or other means of fire stop. In tall buildings, the stack effect can be significant because of the large difference in wind pressure between upper and lower levels of tall buildings due to the shape of the atmospheric boundary layer [44]. This effect can contribute to the acceleration of fire spread through the ventilated gap and should therefore be considered in the analysis. However, for the relatively short building considered in this study, the stack effect is likely minimal and so the simplified approach of modelling the air gap as a solid layer is deemed acceptable.

A single surface is defined in FDS for modelling the external panel, air gap, and PIR insulation simultaneously. The surface is assigned a layered material with thicknesses described in Figure 7 and thermal properties described in Table 1. The use of a single surface to represent a multilayer cladding panel was necessary to reduce the computational cost of the model given the available computing resources. The limitations of this approach should however be taken into account when considering the results of this study.

4.3 Calibrating combustion properties of facade material

There are two methods for modelling the combustion of materials in FDS. This can be done either using pyrolysis models that simulate the chemical decomposition of solid material into combustible gases or by using a simplified approach where combustion parameters are imposed explicitly. The simplified approach is adopted in the current study where combustion properties of ACP are calibrated with data from the DCLG test 1. The calibrated properties include the maximum heat release rate per unit area (HRRPUA) and ignition temperature. A t-squared ramp function is also calibrated to control temporal development of the heat release rate, which was needed to improve fit to experimental data.

Calibration is performed by varying combustion properties until agreement is achieved between temperature profiles from the numerical model and corresponding experimental data. A reasonable agreement was achieved by selecting a maximum heat release rate per unit area of 0.51 MW/m^2 and an ignition temperature of 370 °C. Figure 11 compares temperature plots for thermocouples on the main wall shown in Figure 8c. Aside from locations close to the wing wall, the plots in Figure 11 show reasonable agreement between the FDS model and experiment on the main wall of the facade fire test.

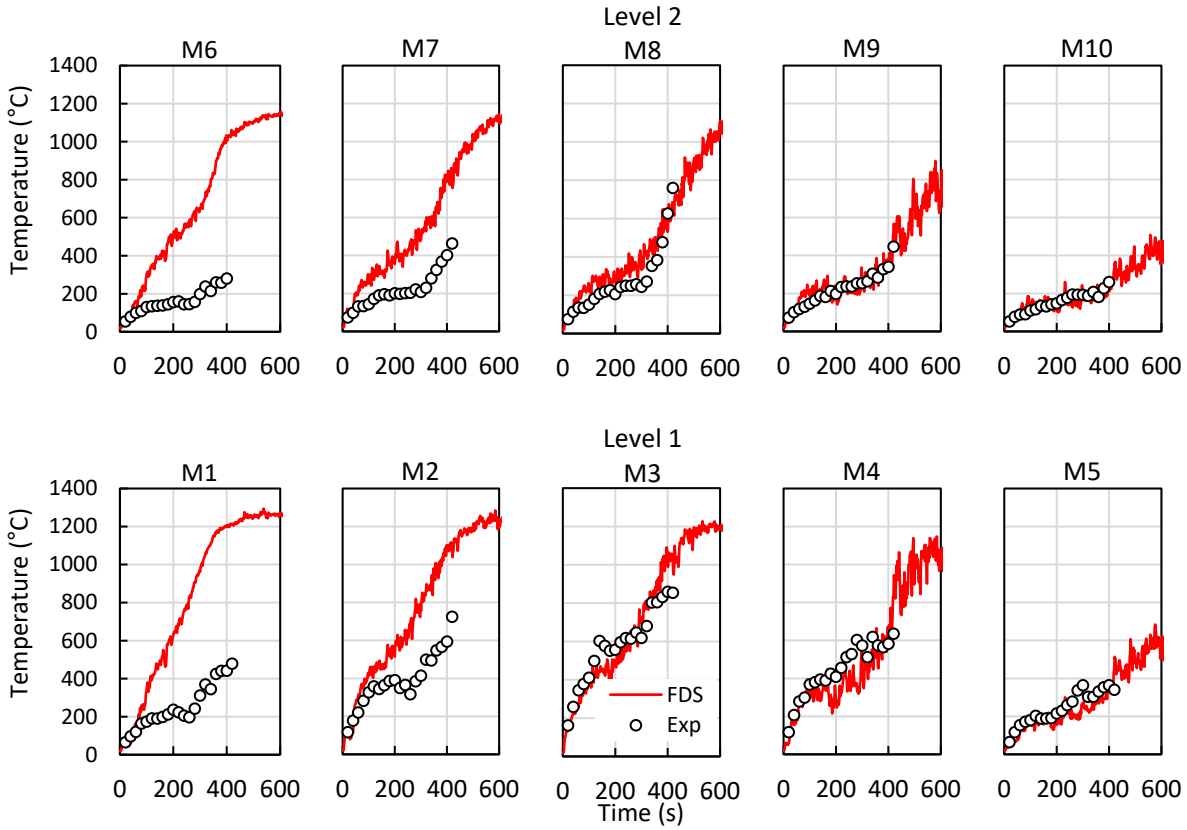

Figure 11: Thermocouple temperatures on the main wall from experiment and FDS model. Thermocouple error is within 0.75% of temperature reading.

There are some limitations of the calibrated material that should be noted. Firstly, the wing wall experienced accelerated fire development compared to the experiment, and it was difficult to calibrate temperature profiles on the main walls and wing wall simultaneously for the simplified material model and coarse grid used. The localised ignition points and the convective heat transfer in the proximity of the joint between the wing wall and main wall may have contributed to this issue. Calibration based on the main wall was nonetheless deemed adequate for the current study considering that the final model involves an external facade that is flush with the fire source. The calibrated material would however not be suitable for cases with complex geometries where the cladding is not flush with the fire source.

An important limitation to consider is the uncertainty associated with the properties of the fire source. The combustion of the wooden crib is not consistent throughout the volume of the crib due to the complex interaction between the combustion of timber and the geometry-dependent ventilation of cold air entering the combustion chamber and hot air leaving the chamber. FDS does not capture well the impact of the geometry when there is a thermal response from the secondary wing, and this contributes to less accurate prediction of temperatures at M1-M2 and M6-M7. Further research is needed to resolve this issue which would lead to improved material calibration of combustible cladding in FDS.

Another limitation of note is the lack of validation data beyond the duration of the experiment. Because the DCLG fire test was performed for testing fire performance, the test was halted once the temperature exceeded performance limits specified by the BS 8414-1 standard. The lack of experimental data beyond this point introduces uncertainty in the behaviour of the fully-developed fire, such as the maximum temperature at which the material burns. This limitation can be addressed

in future studies by performing validation testing where the fire test is continued beyond the point where the facade specimen fails the performance criteria specified in fire testing standards. For the current study, however, the model is deemed adequate for replicating the initial propagation of facade fires as demonstrated by the comparison in Figure 11. The validation of the numerical model could be further improved by including an estimation of experimental uncertainty in the comparison, but this could not be performed in the current study because details of experimental uncertainty are not provided in the DCLG fire test report [38].

5 Parametric study on wind and facade fire interaction

Having validated the wind flow around the building and the combustion properties of the cladding material, the final component of this study involves investigating the effect of wind speed and direction on the propagation of facade fire for an isolated rectangular building described in section 2.1. The calibrated facade material from section 4 is applied to the exterior walls of the building on all sides, while a non-combustible surface is specified at the roof.

To simulate a window-ejected flame, a simple burner surface with dimensions of 2.0 m by 1.0 m is applied to the centre of the building surface at a height of 3.5 m from the ground. The fire source is specified a constant heat release rate of 3.4 MW which is representative of an external flame venting from a fully-developed post-flashover room fire [11]. From preliminary simulations with a non-combustible facade, the heat release rate of the fire source was verified to not be affected by external wind conditions. Hence, it should be noted that this study only addresses wind effects on the combustion of the external facade, and does not account for wind effects on the development of the fire source inside the room.

The atmospheric wind profile described in section 3 is applied to the inlet boundary of the model. Simulation cases are generated by varying the reference wind speed U_{ref} and the direction of the wind. All other parameters of the model are kept constant, including the fire source, material properties, and mesh configuration. The study involves 9 simulation cases as listed in Table 2.

Table 2: List of simulation cases in the parametric study

Number of cases	Wind direction	Wind speeds
1	No wind	
2	Windward	2 m/s, 4 m/s
2	Leeward	2 m/s, 4 m/s
2	Side wind	2 m/s, 4 m/s
2	Diagonal wind	2 m/s, 4 m/s

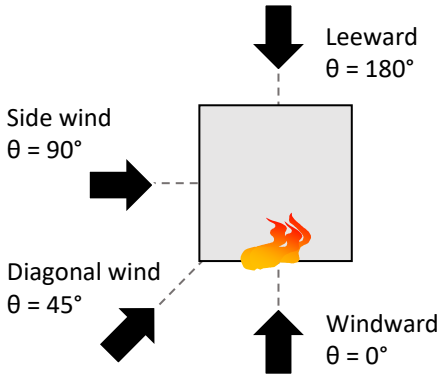

Figure 12: Wind directions relative to fire source (top view)

Four wind directions are considered in the study. These are labelled according to the location of the fire source relative to the approach wind direction (Figure 12). For the windward cases, the fire source is located on the windward surface of the building. Similarly, the fire source is located on the leeward surface for the leeward case. The side wind is only considered from one direction due to the symmetry of the model. The diagonal wind approaches the windward surface of the building at a 45° angle. For each of the wind directions, two highly recurring wind speeds are considered: U_{ref} = 2 m/s and 4 m/s at reference height z_{ref} = 10 m. The 2m/s wind speed aligns closely with the maximum limit in BS 8414-1 standard for facade fire testing. An additional case with no wind is included to serve as a benchmark for investigating the influences of various wind conditions.

Turbulence modelling and near-wall treatment are performed as per the approach described in section 2.3. The simulations are initially solved for 30 s with the fire source deactivated in order to initialise the wind flow field around the building, and further 900 s (15 min) once the fire source was activated. The models are solved on a single computing node with two 6-core Intel (R) Xeon (R) E5-2620 v3 processors at 2.4 GHz and a total RAM of 64 GB. The average CPU time for each case was 34.6 h.

Figure 13 shows simulation results of the instantaneous temperature contours of the facade fire under the different wind conditions considered in this study. For quantitative analysis of fire propagation, a post-processing script was developed using Python 3.8 and the Open-source Computer Vision (OpenCV) library to calculate the time histories of fire spread from contours of wall temperature. Two metrics were used to quantify fire spread:

- **Vertical spread** (meters), calculated as the vertical distance between the fire source (3.5 m above ground) and the highest point on the building surface with a wall temperature greater than 400°C (approx. the ignition temperature of ACP).
- **Fire spread area** (m^2), calculated as the total surface area on the building with a wall temperature greater than 400°C.

The time history of vertical fire spread is presented in the plots on the left in Figure 14, while the fire spread area is presented in the plots on the right. The results in Figure 14 are time-averaged with an averaging period of 30 s.

Figure 15 presents the heat release rate (HRR) from the combustion of the facade material under the various wind conditions considered in this study. The plots are calculated by subtracting the heat release rate of the fire source (3.4 MW) from the total heat release rate in the simulation. Because the HRR of the fire source is assigned using a fixed curve in FDS, the HRR is not expected to be affected by external wind conditions. Preliminary simulations were performed using non-combustible cladding material to verify that the heat release rate of the fire source remained unchanged for all wind conditions considered in this study.

The total energy released by the combustion of the facade is determined by calculating the area under the plots in Figure 15. This provides a convenient metric for quantifying the overall magnitude of the fire using a single value. The results are presented in Figure 16 in units of Gigajoules (GJ).

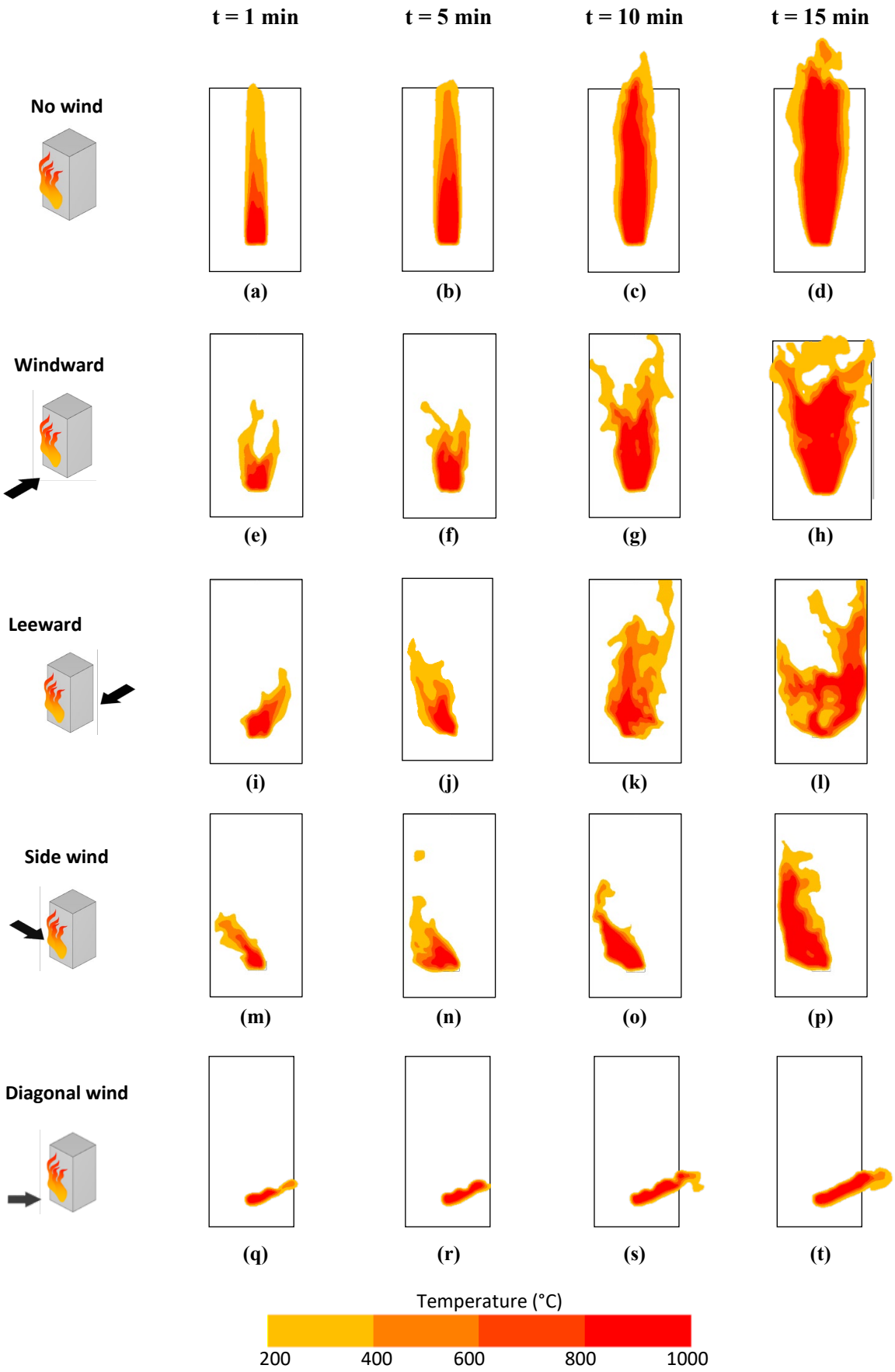

Figure 13: Effect of wind direction on facade fire. Plots show instantaneous temperature contours of external flames at reference wind speed = 4 m/s.

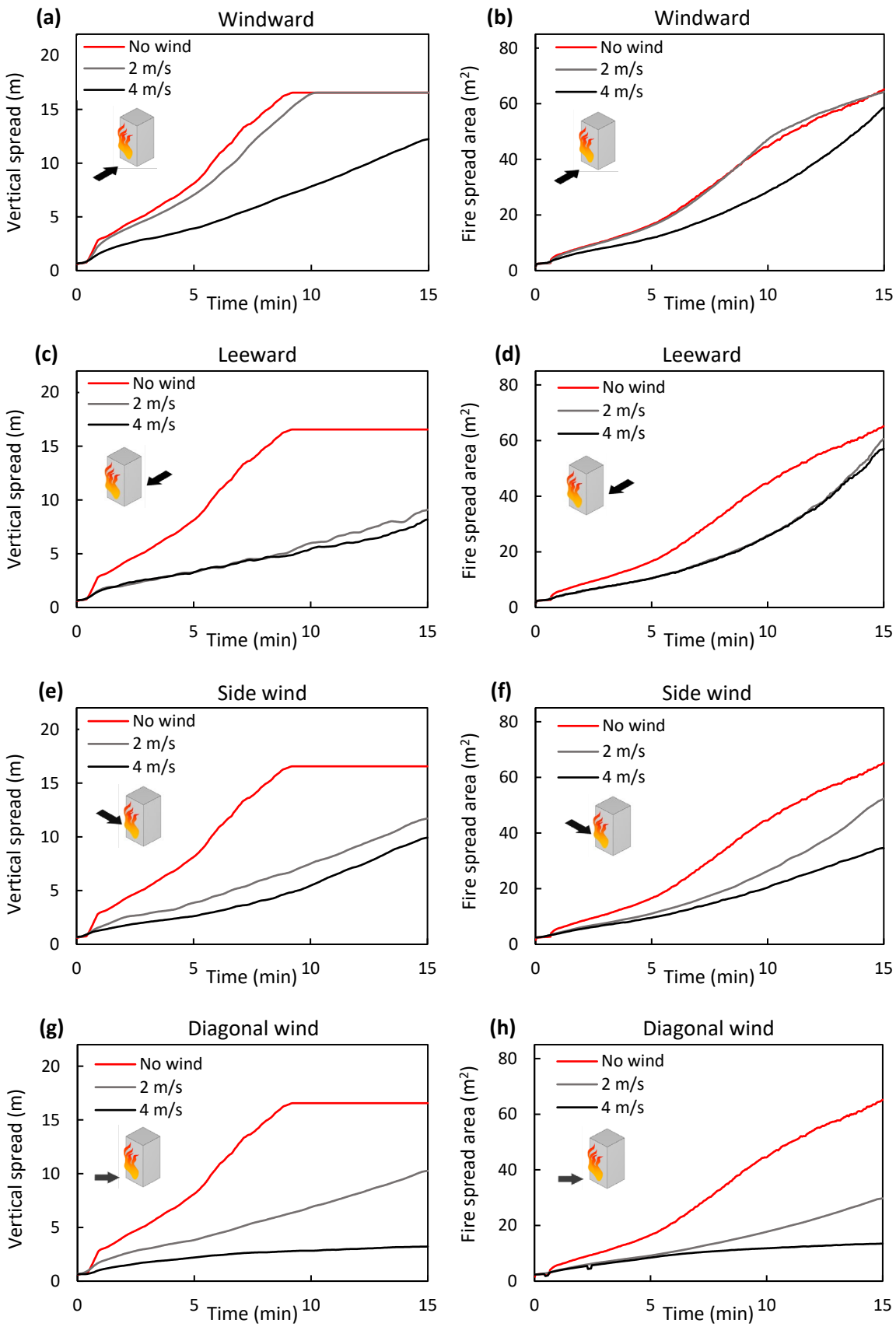

Figure 14: Time histories of facade fire spread under various wind speeds and directions. Plots show vertical fire spread (left) and overall fire spread area (right) on the building surface. Results are time-averaged with an averaging period of 30 s.

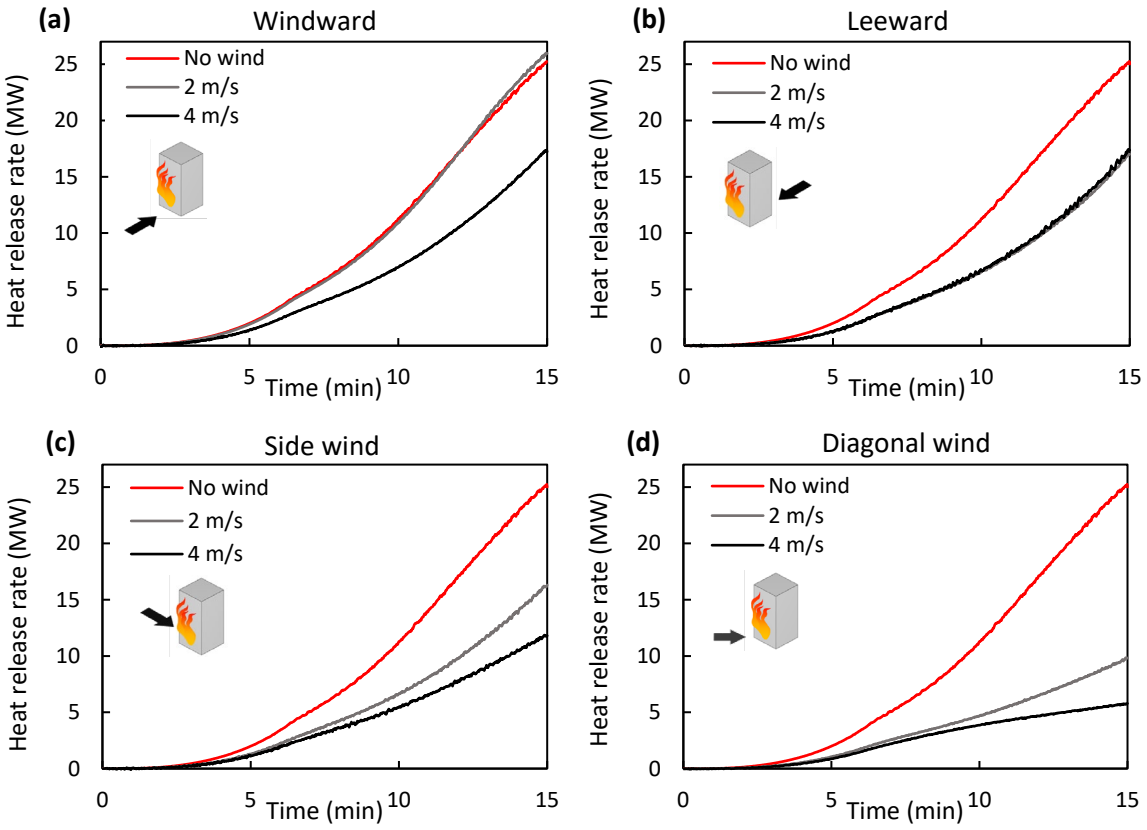

Figure 15: Heat release rate from the combustion of facade panels under various wind speeds and directions

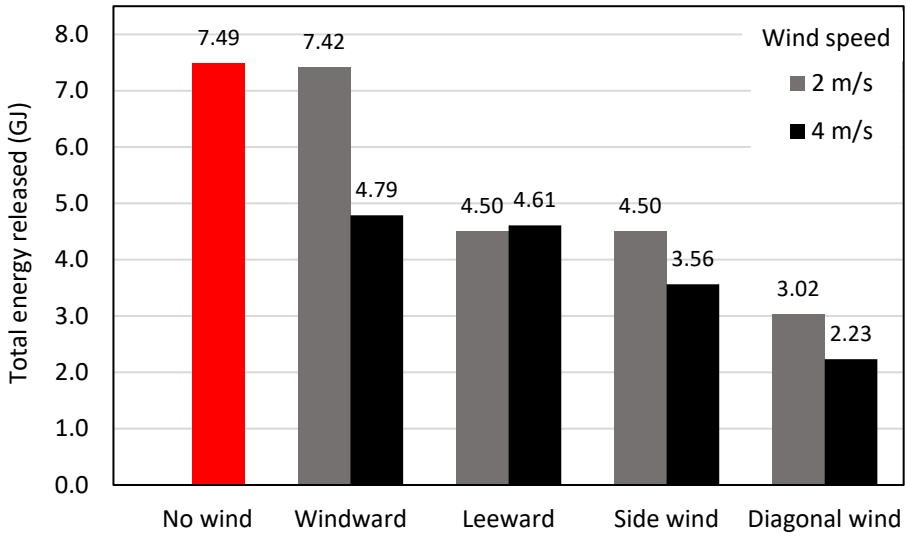

Figure 16: Effect of wind speed and direction on total energy released from the combustion of facade material

6 Results and discussion

The effect of wind conditions on facade fire propagation is investigated by comparing simulation results in section 5 for cases of different wind speeds and directions. The plots of heat release rate (Figure 15) and total energy released (Figure 16) provide an overview of wind effects on the facade fire. Overall, these plots suggest that the presence of external wind causes a reduction in the intensity of the facade fire, with larger wind speeds causing a greater reduction. This indicates that the venting effect [13] is dominant for most wind conditions considered in this study. The largest fire occurred in the case of no wind where the total energy released during the 15-min simulation was 7.49 GJ (Figure 16). This is considerably larger than cases with a wind speed of 4 m/s where the total energy released ranged from 2.23 to 4.79 GJ depending on wind direction.

Although the plots of heat release rate and total energy released provide valuable insight into the overall fire behaviour, a detailed analysis of facade fire propagation under wind effects can be performed by examining results of temperature contours of the external flame (Figure 13) and plots of vertical spread and fire spread area (Figure 14). These results are discussed in detail in the following subsections.

6.1 Benchmark case with no wind

Of all cases considered in this study, the benchmark case with no wind resulted in the fastest vertical spread of the fire (Figure 14a), although the fire spread was mostly limited to the centre of the building surface (Figure 13a-d). It took approximately 9 min for the fire to reach the top of the building (average vertical spread rate = 1.9 m/min), and by the end of the simulation (15 min), approximately 32% of the frontal surface area (63.1 m^2) was experiencing temperatures above 400°C. The lack of external wind seems to provide highly favourable conditions for vertical buoyant forces to drive the flame upwards along the building facade.

The vertical spread rate for the no wind case (1.9 m/min) is lower than that observed in the initial stages of the Grenfell Tower fire (3.6 m/min) where the same cladding material was used [45]. This discrepancy could be explained by differences in the heat release rate of the initial fire source. The initial fire in the Grenfell incident was estimated to be as high as 4 MW [46] which is greater than the 3.4 MW fire used in this study. This may have contributed to the greater vertical spread rate in the Grenfell fire. Despite this discrepancy, the vertical spread rate achieved in this study is still a reasonable reflection of an ACP facade fire given that it falls within the uncertainty range given for the quantitative analysis of the Grenfell fire by Guillaume et al. [45].

6.2 Effect of perpendicular wind

Results from the windward cases indicate that external wind acting perpendicular to the fire source causes an initial delay in the vertical spread of the fire (Figure 13e-f). This delay is influenced by wind speed. As shown in Figure 14a, a wind speed of 2 m/s resulted in a minor delay compared to the case of no wind (10 min to reach the top of the building), while a wind speed of 4 m/s resulted in a considerable delay and reduction in the total vertical spread. At t = 15 min, the total vertical spread was 16.6 m for both the no wind case and for 2 m/s wind, while the 4 m/s case had a total vertical spread of 12.2 m. This corresponds to a 26% reduction in total vertical propagation for the 4 m/s case.

The reduction in vertical fire propagation under perpendicular wind may be attributed to the formation of a high-pressure stagnation region on the windward surface that could inhibit the initial spread of

the flame as seen in Figure 13e-f. Moreover, the presence of perpendicular wind may have generated a downdraft on the windward surface that counteracts the vertical buoyant forces generated by the fire plume, thereby reducing the speed of vertical fire propagation. This finding aligns with previous research that reports a reduction in flame height under perpendicular wind [13, 14].

Despite a reduction in vertical propagation, the windward case of 4 m/s experienced only a minor reduction in the total area of fire spread. Figure 14b shows that at 15 min, the total area on the facade with temperatures greater than 400°C was 65.2 m^2 for the cases of no wind and 2 m/s, while the case of 4 m/s showed only a marginal reduction (< 5%) with a fire spread area of 58.4 m^2. The windward case of 4 m/s experienced greater lateral fire spread towards the side edges of the building compared to the case with no wind (Figure 13h). The lateral spread is likely due to the behaviour of the approaching wind that, once blocked by the presence of the building, is forced to travel around the side edges and above the top edge at accelerated speeds carrying the flames with it.

Hence, perpendicular wind tends to inhibit the vertical spread of fire while increasing the lateral spread along the windward surface; however, the extent of this influence is largely dictated by the wind speed.

6.3 Effect of leeward wake

In the leeward cases, the wind is approaching from the opposite direction of the fire source, so the facade fire occurs on the leeward surface that is encompassed by the wake of the building. Figure 14c indicates that the leeward wake resulted in a considerable reduction in vertical fire propagation. For wind speeds of 2 m/s and 4 m/s, the maximum vertical spread at 15 min was 9.4 m and 8.4 m, respectively. This represents a 43-48% reduction in total vertical spread compared to the case of no wind. This is likely due to large negative pressures in the wake region causing the fire to be drawn away from the building surface, thereby resulting in a reduction of vertical fire spread.

Despite a considerable reduction in vertical spread, the leeward cases experienced a large amount of lateral spread which resulted in an overall fire spread area that is comparable to the no wind case at 15 min (Figure 14d). The lateral spread of fire in the leeward wake is likely driven by the vortex shedding phenomenon that causes the fire plume to fluctuate back and forth as shown in Figure 17. The frequency of vortex shedding is known to be influenced by many factors including wind speed and building shape and size. However, it is not clear how changes in vortex shedding behaviour will affect facade fire propagation. This is an important issue to consider in taller buildings where stronger vortex shedding behaviour is more likely to occur.

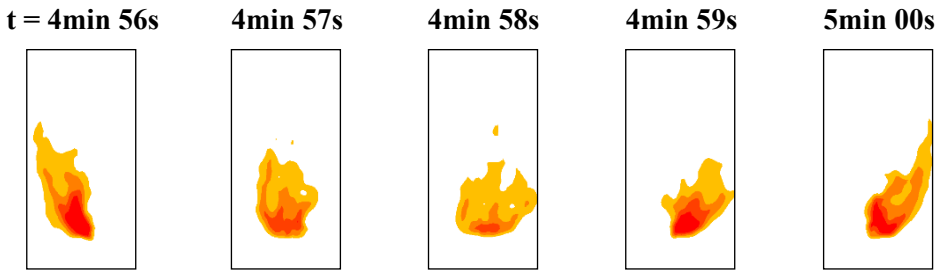

Figure 17: Side-to-side fluctuation of facade fire in leeward wake during a 5 s period. Reference wind speed = 4 m/s.

Although the shedding of vortices is known to be influenced by wind speed, this seems to have a minimal effect on fire spread behaviour for the building considered in this study. Figure 14c-d shows similar plots for wind speeds of 2 m/s and 4 m/s. At t = 15 min, the higher wind speed of 4 m/s only resulted in a marginal reduction of vertical spread (< 10%) and total spread area (< 5%) compared to the 2 m/s case.

Overall, the results indicate that the leeward wake is likely to reduce the vertical propagation of facade fire considerably, while only marginally reducing the overall fire spread area due to increased lateral spread. Moreover, fire spread in the leeward wake is not significantly affected by wind speed.

6.4 Effect of side wind

The presence of side wind caused a reduction in the vertical spread and total fire spread area compared to the case of no wind (Figure 14e-f). Interestingly, the presence of side wind caused the flame to tilt in the opposite direction to the approaching wind (Figure 13m-p). This contradicts findings in the literature that report tilting of the flame in the direction of the side wind in facade test sections [15-19]. Nonetheless, this behaviour can be explained by the flow structures generated at the sides of the rectangular building (Figure 2). Flow separation that occurs at the leading edges creates large wake regions on the sides of the building with large negative pressures occurring immediate downstream the leading corners. The large negative pressures produce a recirculating flow that draws the flame towards the leading edge of the building (Figure 18a). This behaviour of reverse flow in the wake region is a well-established phenomenon in wind-engineering literature [47-50]. Notably, the fire is unable to spread beyond the leading edge (left edge in Figure 13m-p) due to the presence of a strong streamwise wind shear layer at that location. The flames spread upwards once they reach the leading edge.

The discrepancy between the current findings and previous studies can be explained by differences in the geometries being considered and resulting differences in the size of the wake regions. Previous studies on side wind were performed for thin facade sections which are expected to generate minimal flow separation and smaller side wakes. In such cases, the fire is expected to tilt towards the downwind direction under the influence of side wind rather than experiencing large negative pressures that draw the flame toward the upwind direction as seen in the rectangular building of this study. These results highlight the importance of including the full building geometry and resulting flow fields when assessing wind effects on facade fires.

It should be noted that the results of fire spread under side wind may have been affected to some extent by limitations of the FDS model in replicating the flow field near the side walls as described previously. Despite the FDS model underpredicting the size of the wake region, the generated wake was still sufficient to fully encompass the side walls of the rectangular building and to produce the distinctive reverse-flow behaviour seen in Figure 18a. This suggests that the general behaviour of fire spread under side wind was not affected by limitations of the FDS model, although further improvement to flow field predictions in FDS is needed to improve confidence in the quantitative results.

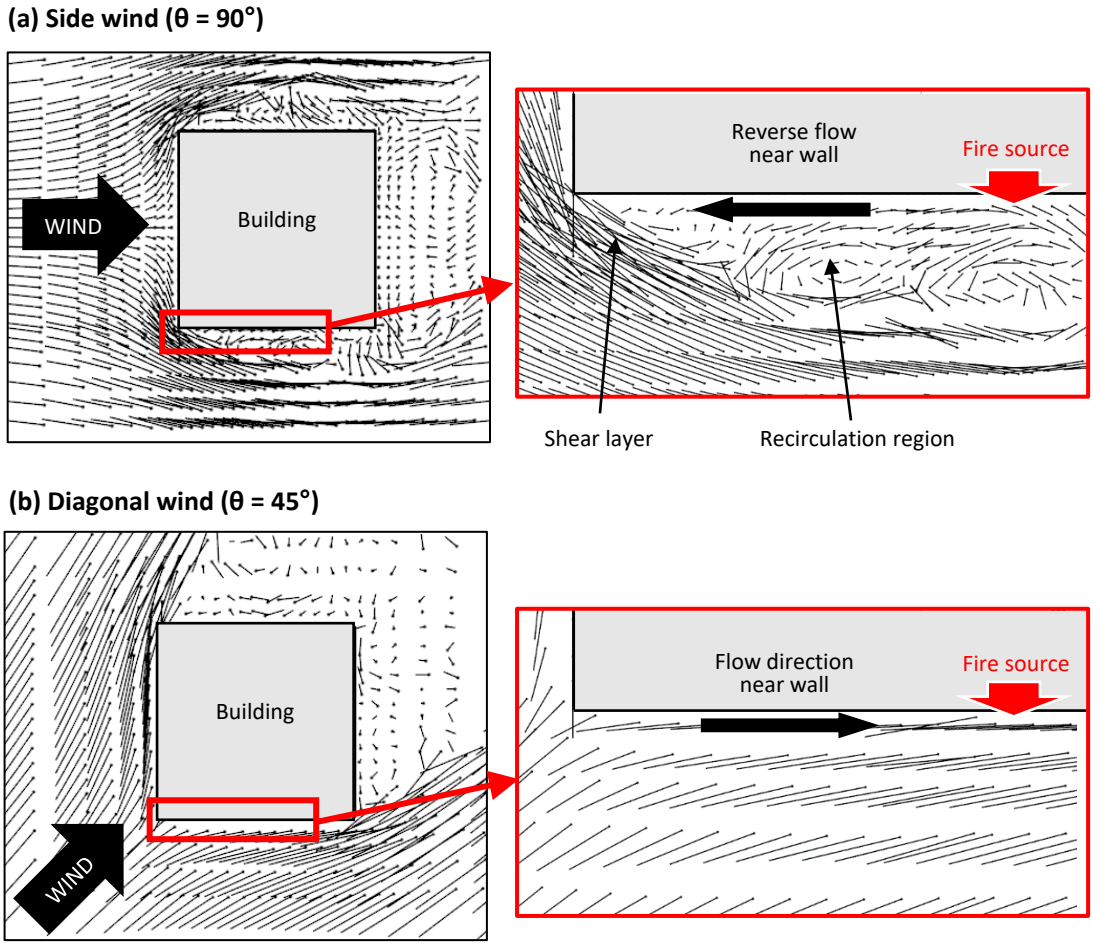

Figure 18: Top view of flow past building at z/H = 0.625 for cases of (a) side wind and (b) diagonal wind. Close-up view of flow near the fire source is shown on right.

6.5 Effect of diagonal wind

The case of diagonal wind experiences very different behaviour to side wind. The lack of flow separation for the diagonal case results in an undisturbed and streamlined parallel flow near the building surface (Figure 18b). As a result, the fire plume experiences very strong tilting in the direction of the wind (Figure 13q-t). This behaviour is consistent with studies on side wind in facade test sections [15-19].

For the diagonal cases, the wind speed seems to have a considerable influence on the rate of vertical and overall fire spread (Figure 14g-h). The case of 4 m/s experienced the lowest fire spread of all cases considered in this study with a maximum vertical spread of 3.2 m and a total spread area of 13.5 m^2 at 15 min. The case of 2 m/s experienced considerably larger values of fire spread compared to 4

m/s with a vertical spread of 10.3 m and a total spread area of 30.1 m^2 at 15 min. However, these values are still considerably lower than the benchmark case of no wind. Hence, it may be concluded that larger wind speeds for the diagonal cases reduce the risk of fire propagation. However, the strong tilting of the flame towards the downwind direction as seen in Figure 13t could potentially lead to further spread of fire to the side surfaces of the building.

6.6 Increased risk of fire propagation under variable wind conditions

The results presented so far indicate that the presence of external wind is likely to inhibit fire spread during the initial stages of facade fire development. These cases were performed with constant wind conditions that are present from the initial ignition of the facade and remain unchanged for the entire duration of the simulation. Under such conditions, the presence of any combination of wind speed and direction was seen to reduce the risk of fire propagation compared to the case of no wind. However, real wind conditions can vary with time and this can potentially increase the risk of fire propagation. To demonstrate this point, an additional case is performed with variable wind conditions that are likely to increase the risk of facade fire propagation. These conditions were selected based on the findings of this study with the aim of maximising fire spread. The simulation is performed for a total duration of 30 min divided into three segments as follows:

- **t = 0 - 10 min:** no wind to allow for initial fire development (Figure 19a)
- **t = 10 – 20 min:** diagonal wind with θ = 45° and U_{ref} = 4 m/s (Figure 19b)
- **t = 20 – 30 min:** wind direction is changed to θ = -45° while wind speed is unchanged at U_{ref} = 4 m/s (Figure 19c)

The results of the variable wind case are presented in Figure 19, where it can be seen that the lack of external wind from t = 0 - 10 min causes the fire to spread vertically (Figure 19a) at a rate equivalent to that of the no wind case (Figure 19d). As a diagonal wind is introduced at t = 10 min, the vertical plume that has already developed experiences lateral spread to the downwind direction. This causes the fire to reach the trailing edge of the building and spread to the side wall (Figure 16b). At t = 20 min, the total fire spread area for the variable wind case has increased by 17 % compared to the case of no wind (Figure 19d).

As wind conditions are varied again at t = 20 min, the fire undergoes further lateral spread on the main wall but in the opposite direction, reaching the left edge of the building (Figure 19c). The wind also causes further lateral spread of fire on the side wall that has now fully ignited. This increases the total fire spread area on the building facade from 113.1 m^2 for the case of no wind to 170.1 m^2 for the case of variable wind, which represents a 50% increase in total fire spread area at t = 30 min.

An animated comparison of fire spread for variable wind and no wind cases is presented in Appendix A.

The variable wind conditions in this study have been specifically selected to maximise fire spread, but these conditions are not unrealistic. The results clearly demonstrate the potential of a synergistic effect and a resulting increased risk of facade fire spread under variable wind conditions. These effects should be considered when assessing the fire safety of buildings.

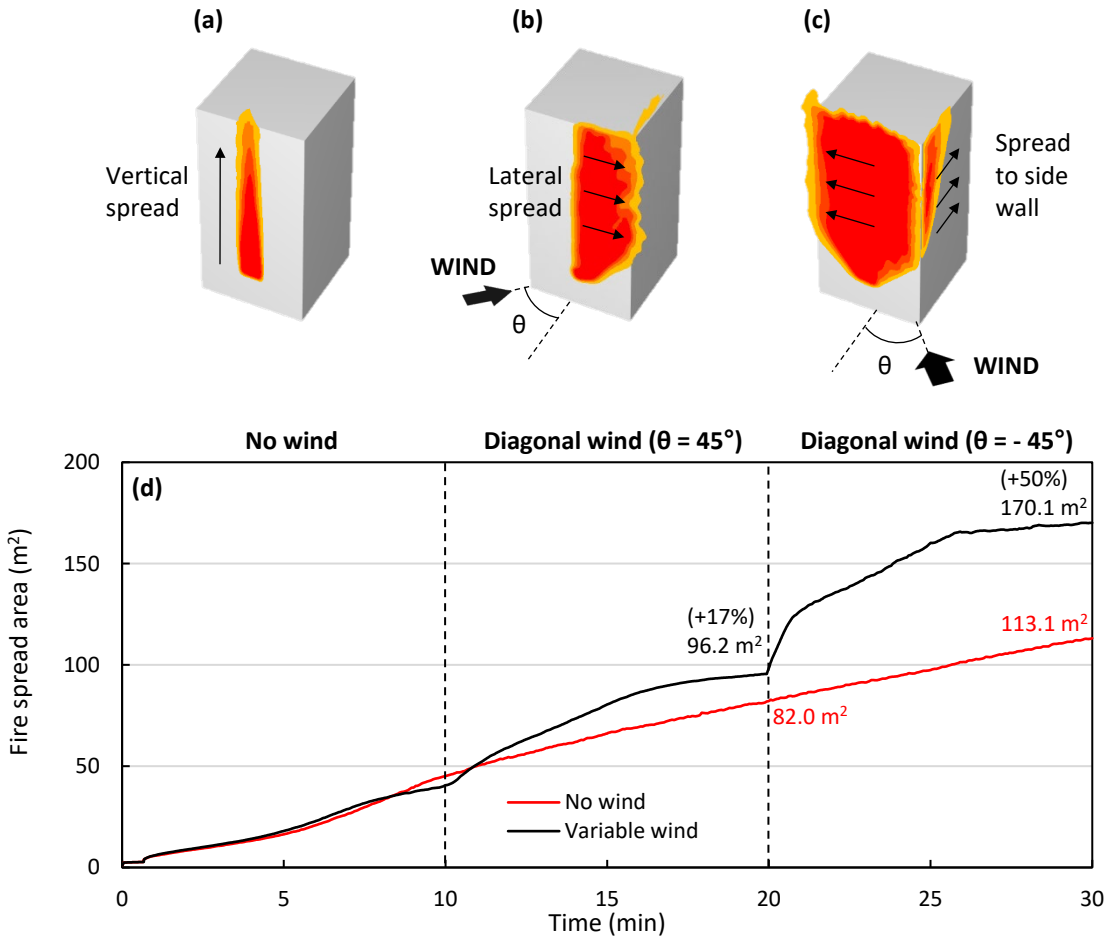

Figure 19: Fire spread on building facade under variable wind conditions at (a) t = 10 min, (b) t = 20 min, and (c) t = 30 min. Plot (d) compares the fire spread area on the building surface with temperatures greater than 400°C.

7 Conclusions

This study investigated the influence of wind speed and direction on the propagation of facade fires in an isolated rectangular building. A computational fluid dynamics (CFD) model was constructed in Fire Dynamics Simulator (FDS) and validated with experimental data from wind tunnel and facade fire tests. A series of parametric studies with four wind directions and two wind speeds were performed with the validated model. The main conclusions from this study are summarized as follows:

- Wind flow patterns generated by the building geometry were found to dictate the behaviour of facade fire propagation. The full building geometry and resulting wind flow patterns need to be considered when assessing wind effects on facade fires.
- Both wind speed and direction have a considerable influence on facade fire propagation. The case of no wind experienced the quickest vertical propagation but with minimal lateral spread. Perpendicular wind inhibits the vertical spread of fire while increasing the lateral spread along the windward surface. The leeward wake region generates highly unstable conditions that increase the lateral fire spread while reducing vertical propagation.
- For the rectangular building considered in this study, side wind caused the fire to spread laterally in a direction opposite to the wind flow, while diagonal wind caused a very strong

lateral spread in the downwind direction. These behaviours are explained by differences in near-wall flow structures generated under the influences of side and diagonal winds.

- There is a synergistic effect on the spread of facade fires with variable wind conditions. Once the fire has fully developed; the presence of wind can considerably increase the risk of fire spread along multiple facade surfaces on the building. Variable wind conditions need to be considered when assessing the fire safety of buildings.

The study reveals interesting aspects of wind and fire interaction that could contribute to reduced fire safety performance in building facades. Most notably, the increase in lateral fire spread due to side wind and diagonal wind can potentially reduce the effectiveness of fire protection features such as overhangs and balconies as lateral spread can cause the fire to penetrate the space between these protective features. Further research is needed to investigate the performance of these safety features under temporally varying wind conditions and for complex building geometries.

Due to the large number of parameters included in this study and limitations in available computing resources, the study only considered a limited range of wind speeds and directions. Although these were sufficient to provide an insight into the general behaviour of wind and fire interaction under highly recurrent wind speeds, further research is needed to consider intermediate values of wind speeds and direction not considered in this study, as well as considering the effect of extreme wind events.

A notable limitation of the study is the use of a simplified approach for modelling the ACP material, where a single surface was used to model the entire cladding system. This approach has considerable limitations as it does not account for the combustion of individual cladding components and excludes the modelling of fire spread in the air gap between the ACP panel and the insulation layer. The simplified material was calibrated to replicate the general fire spread behaviour of ACP which was deemed adequate for the purpose of investigating wind and fire interaction at the full building scale. This limitation should however be addressed in a future study with more intricate models of ACP and other cladding systems.

The study assumed a fully-developed, post-flashover flame as the fire source for the initial ignition of the facade. The study does not account for the effect of external wind on the initial development of the localised fire inside the room, and further research is needed to include this effect in the model. The study also does not account for the development of secondary fires caused by the re-entry of the external flame through openings. Modelling these behaviours requires accounting for the interactions between external and internal parameters which considerably increases the complexity of the model. The influence of secondary fires on facade fire spread under wind effects is an important area for future research.

Further research is also needed to investigate other parameters not considered in this study including the effect of inflow turbulence and turbulence generated by nearby structures, as well as the influence of the stack effect within the ventilation gap between the exterior facade panel and internal insulation. These will improve confidence in the fire safety performance of building facades under various wind conditions.

Funding sources

This work was supported by the Australian Research Council [grant numbers: DE190100217 - Facade fire failures in buildings: a robust nanocomposite solution, IH200100010 - Transformation of Reclaimed Waste Resources to Engineered Materials and Solutions for a Circular Economy TREMS, and CRCPEIGHT00084 - Upcycling solutions for hazardous cladding and co-mingled waste].

Appendix A. Supplementary data

[INSERT LINK TO VIDEO HERE]

Video caption: Side-by-side comparison of fire spread under no wind and variable wind conditions.

References

1. Nguyen, K.T., et al., *Performance of modern building façades in fire: a comprehensive review.* Electronic Journal of Structural Engineering, 2016. **16**(1): p. 69-86.
2. Bonner, M. and G. Rein, *Flammability and multi-objective performance of building façades: towards optimum design.* International Journal of High-Rise Buildings, 2018. **7**(4): p. 363-374. https://doi.org/10.21022/IJHRB.2018.7.4.363.
3. Spinardi, G. and A. Law, *Beyond the stable door: Hackitt and the future of fire safety regulation in the UK.* Fire Safety Journal, 2019. **109**: p. 102856. https://doi.org/10.1016/j.firesaf.2019.102856.
4. Bisby, L., *Grenfell Tower Inquiry report. Phase 1: Expert report*. 2018.
5. Genco, G., *Lacrosse Building Fire: 673 La Trobe Street, Docklands on 25 November 2014*. 2015, City of Melbourne: Melbourne, Australia.
6. Węgrzyński, W. and T. Lipecki, *Wind and Fire Coupled Modelling—Part I: Literature Review.* Fire Technology, 2018. **54**(5): p. 1405-1442. https://doi.org/10.1007/s10694-018-0748-5.
7. Pitts, W.M., *Wind effects on fires.* Progress in Energy and Combustion Science, 1991. **17**(2): p. 83-134. https://doi.org/10.1016/0360-1285(91)90017-H.
8. Canton, L.G., *San Francisco 1906 and 2006: An Emergency Management Perspective.* Earthquake Spectra, 2006. **22**(2_suppl): p. 159-182. https://doi.org/10.1193/1.2181467.
9. Suzuki, S. and S.L. Manzello, *Characteristics of Firebrands Collected from Actual Urban Fires.* Fire Technology, 2018. **54**(6): p. 1533-1546. https://doi.org/10.1007/s10694-018-0751-x.
10. International Organization for Standardization, *ISO 13785-2:2002 : Reaction-to-fire tests for facades - Part 2: Large-scale test*. 2002.
11. British Standards Institution, *BS 8414-1:2015 + A1:2017 - Fire performance of external cladding systems. Test methods for non-loadbearing external cladding systems applied to masonry face of a building*. 2017.
12. Standards Australia, *AS 5113:2016 - Fire propagation testing and classification of external walls of buildings*. 2016, SAI Global Limited: Sydney.
13. Hu, L., et al., *Facade flame height ejected from an opening of fire compartment under external wind.* Fire Safety Journal, 2017. **92**: p. 151-158. https://doi.org/10.1016/j.firesaf.2017.06.008.
14. Fang, X., et al., *Facade flame height ejected from opening of a compartment under the coupling effect of side walls and ambient wind.* Fire Safety Journal, 2020. **112**: p. 102966. https://doi.org/10.1016/j.firesaf.2020.102966.
15. Bai, Z.P., Y.F. Li, and Y.H. Zhao, *Study on characteristics of fire plume in building facade window under lateral blow.* PLoS ONE, 2019. **14**(11): p. e0225120. https://doi.org/10.1371/journal.pone.0225120.

16. Hu, L., et al., *Facade flame height and horizontal extending distance from opening of compartment fire with external sideward wind.* Proceedings of the Combustion Institute, 2019. **37**(3): p. 3859-3867. https://doi.org/10.1016/j.proci.2018.06.201.

17. Li, J., et al. *Side wind effect on the flow behavior of the window plume*. in *Asia-Oceania Symposium on Fire Science and Technology*. 2018. Springer. https://doi.org/10.1007/978-981-32-9139-3_9.

18. Li, J.M., et al. *Computational study of wind effect on window flame spread across the exterior wall of high-rise building*. in *Applied Mechanics and Materials*. 2013. Trans Tech Publications. https://doi.org/10.4028/www.scientific.net/AMM.438-439.1898.

19. Sugawa, O., D. Momita, and W. Takahashi, *Flow behavior of ejected fire flamelplume from an opening effected by external side wind.* Fire Safety Science, 1997. **5**: p. 249-260. https://doi.org/10.3801/IAFSS.FSS.5-249.

20. Wang, T.-h., H. Zhao, and Y. Zhou, *Analysis on the influence of fire overhangs on the window to exterior wall vertical fire plume spreading under external wind.* Procedia Engineering, 2016. **135**: p. 384-392. https://doi.org/10.1016/j.proeng.2016.01.146.

21. Ren, F., L. Hu, and X. Sun, *Experimental investigation on lateral temperature profile of window-ejected facade fire plume with ambient wind.* Fire Technology, 2019. **55**(3): p. 903-913. https://doi.org/10.1007/s10694-018-0809-9.

22. Ren, F., et al., *An experimental study on vertical temperature profile of facade fire plume ejected from compartment with an opening subjected to external wind normal to facade.* International Journal of Thermal Sciences, 2018. **130**: p. 94-99. https://doi.org/10.1016/j.ijthermalsci.2018.04.008.

23. Gao, W., et al., *Fire spill plume from a compartment with dual symmetric openings under cross wind.* Combustion and Flame, 2016. **167**: p. 409-421. https://doi.org/10.1016/j.combustflame.2016.01.011.

24. Cao, L. and Y. Guo, *Large eddy simulation of external fire spread through openings.* International Journal on Engineering Performance-based Fire Codes, 2003. **5**(4): p. 176-180.

25. Li, M., et al., *Wind effects on transition and extension characteristics of the external flame projecting from a compartment with opposing openings.* Fire Safety Journal, 2020: p. 103102. https://doi.org/10.1016/j.firesaf.2020.103102.

26. Li, M., et al., *Wind effects on flame projection probability from a compartment with opposing openings.* Fire Safety Journal, 2017. **91**: p. 414-421. https://doi.org/10.1016/j.firesaf.2017.04.037.

27. Zheng, L., et al. *Influence of Wind Direction on Fire Spread on the Exposed XPS insulation Wall*. in *IOP Conference Series: Earth and Environmental Science*. 2020. IOP Publishing. https://doi.org/10.1088/1755-1315/526/1/012013.

28. Abu-Zidan, Y.F., *Verification and validation framework for computational fluid dynamics simulation of wind loads on tall buildings*, in *Department of Infrastructure Engineering*. 2019, The University of Melbourne. https://doi.org/11343/228846.

29. Węgrzyński, W., T. Lipecki, and G. Krajewski, *Wind and Fire Coupled Modelling—Part II: Good Practice Guidelines.* Fire Technology, 2018. **54**(5): p. 1443-1485. https://doi.org/10.1007/s10694-018-0749-4.

30. McGrattan, K., et al., *Fire dynamics simulator user's guide.* NIST special publication, 2019. **1019**(6).

31. Abu-Zidan, Y., P. Mendis, and T. Gunawardena, *Impact of atmospheric boundary layer inhomogeneity in CFD simulations of tall buildings.* Heliyon, 2020. **6**(7): p. e04274. https://doi.org/10.1016/j.heliyon.2020.e04274.

32. Abu-Zidan, Y., P. Mendis, and T. Gunawardena, *Optimising the computational domain size in CFD simulations of tall buildings.* Heliyon, 2021. **7**(4): p. e06723. https://doi.org/10.1016/j.heliyon.2021.e06723.

33. Smagorinsky, J., *General circulation experiments with the primitive equations: I. The basic experiment.* Monthly Weather Review, 1963. **91**(3): p. 99-164. https://doi.org/10.1175/1520-0493(1963)091<0099:GCEWTP>2.3.CO;2.

34. Okaze, T., et al., *Benchmark test of flow field around a 1:1:2 shaped building model using LES: Influences of various calculation conditions on simulation result.* AIJ Journal of Technology and Design, 2020. **26**(62): p. 179-184. https://doi.org/10.3130/aijt.26.179.

35. Pope, S.B., *Turbulent Flows*. 2000, Cambridge: Cambridge University Press.

36. Nicoud, F. and F. Ducros, *Subgrid-scale stress modelling based on the square of the velocity gradient tensor.* Flow, Turbulence and Combustion, 1999. **62**(3): p. 183-200. https://doi.org/10.1023/A:1009995426001.

37. Meng, Y. and K. Hibi, *Turbulent measurements of the flow field around a high-rise building.* Wind Engineers, JAWE, 1998(76): p. 55-64. https://doi.org/10.5359/jawe.1998.76_55.

38. BRE Global Ltd, *Report No B 137611-1037 (DCLG test 1)*. 2017.

39. Dréan, V., et al., *Numerical simulation of the fire behaviour of facade equipped with aluminium composite material-based claddings - Model validation at large scale.* Fire and Materials, 2019. **43**(8): p. 981-1002. https://doi.org/10.1002/fam.2759.

40. Dréan, V., et al., *Numerical simulation of the fire behaviour of façade equipped with aluminium composite material-based claddings - Model validation at intermediate scale.* Fire and Materials, 2019. **43**(7): p. 839-856. https://doi.org/10.1002/fam.2745.

41. Periodic Table. *Aluminium – Periodic Table*. 2020; Available from: https://www.periodic-table.org/Aluminium-periodic-table/.

42. Xometry, *Datasheet: HDPE (High Density Polyethylene)*. 2021.

43. Drean, V., R. Schillinger, and G. Auguin, *Assessment of an insulating air layer model of façade external system: contribution to fire simulation of facade performance fire test.* Journal of Physics: Conference Series, 2018. **1107**: p. 042004. https://doi.org/10.1088/1742-6596/1107/4/042004.

44. Mijorski, S. and S. Cammelli, *Stack effect in high-rise buildings: a review.* International Journal of High-Rise Buildings, 2016. **5**(4): p. 327-338. https://doi.org/10.21022/IJHRB.2016.5.4.327.

45. Guillaume, E., et al., *Reconstruction of Grenfell Tower fire. Part 1: Lessons from observations and determination of work hypotheses.* Fire and Materials, 2020. **44**(1): p. 3-14. https://doi.org/10.1002/fam.2766.

46. Guillaume, E., et al., *Reconstruction of Grenfell Tower fire. Part 2: A numerical investigation of the fire propagation and behaviour from the initial apartment to the façade.* Fire and Materials, 2020. **44**(1): p. 15-34. https://doi.org/10.1002/fam.2765.

47. Castro, I.P. and A.G. Robins, *The flow around a surface-mounted cube in uniform and turbulent streams.* Journal of Fluid Mechanics, 1977. **79**(2): p. 307-335. 10.1017/S0022112077000172.

48. Martinuzzi, R. and C. Tropea, *The Flow Around Surface-Mounted, Prismatic Obstacles Placed in a Fully Developed Channel Flow (Data Bank Contribution).* Journal of Fluids Engineering, 1993. **115**(1): p. 85-92. 10.1115/1.2910118.

49. Ogawa, Y., S. Oikawa, and K. Uehara, *Field and wind tunnel study of the flow and diffusion around a model cube—II. Nearfield and cube surface flow and concentration patterns.* Atmospheric Environment (1967), 1983. **17**(6): p. 1161-1171. https://doi.org/10.1016/0004-6981(83)90339-6.

50. Paterson, D.A. and C.J. Apelt, *Simulation of flow past a cube in a turbulent boundary layer.* Journal of Wind Engineering and Industrial Aerodynamics, 1990. **35**: p. 149-176. https://doi.org/10.1016/0167-6105(90)90214-W.